

Unidirectional and Single-File Diffusion of Molecules in One-Dimensional Channel Systems. A Quasi-Elastic Neutron Scattering Study

Hervé Jobic,^{*,†} Karsten Hahn,[‡] Jörg Kärger,[‡] Marc Bée,[§] Alain Tuel,[†] Manfred Noack,^{||} Irina Girnus,^{||} and Gordon J. Kearley[⊥]

Institut de Recherches sur la Catalyse, CNRS, 2 Avenue Albert Einstein, 69626 Villeurbanne, France, Fakultät für Physik und Geowissenschaften, Universität Leipzig, Linnéstrasse 5, 04103 Leipzig, Germany, Laboratoire de Spectrométrie Physique, Université Joseph Fourier, 38402 St. Martin d'Hères, France, Institut für Angewandte Chemie, Rudower Chaussee 5, 12484 Berlin, Germany, and Institut Laue-Langevin, BP 156, 38042 Grenoble, France

Received: March 3, 1997; In Final Form: May 23, 1997[⊗]

Translational diffusion of molecules in one-dimensional channel systems has been measured by quasi-elastic neutron scattering. The scattering function for a single-file diffusion model has been derived in order to differentiate this transport model from normal 1D diffusion. In the AlPO₄-5 structure, ordinary 1D diffusion is observed for methane and ethane, whatever the loading, which indicates that the molecules are able to pass each other. The diffusion coefficients for both molecules are on the order of 10⁻⁹ m² s⁻¹. On the other hand, a quite different regime is obtained by varying cyclopropane concentration in the same structure. At low loading, normal 1D diffusion is observed because the molecules can be considered as isolated, but at higher concentration cyclopropane is found to follow single-file diffusion. However, the mobility is too small to be determined. In the less open channel system of ZSM-48, ordinary 1D diffusion is found for small methane concentration, the diffusion coefficient being 2.5 × 10⁻⁹ m² s⁻¹, at 155 K. At medium loading, single-file diffusion is observed with a mobility factor of 2 × 10⁻¹² m² s^{-1/2}. This is the first time that this technique has provided experimental evidence of single-file diffusion in zeolites.

Introduction

The catalytic and separation properties of zeolites are critically dependent on diffusion and molecular sieving effects. In particular, modeling the performance of zeolite membranes requires a detailed description of gas adsorption and transport at the microscopic level. Therefore, much effort is still devoted to measuring diffusion coefficients in zeolites and to try to understand the discrepancies between the different techniques.¹ The two methods that are now available to elucidate the mechanism of diffusion inside zeolite crystals are pulsed-field gradient NMR (PFG NMR) and quasi-elastic neutron scattering (QENS). These two methods are complementary in that molecular migration is followed over a few unit cells with QENS (time scale ≈ 1 ns) and over the whole crystal with PFG NMR (time scale ≈ 1 ms).

The regular structure of zeolite frameworks has allowed molecular dynamics (MD) simulations to be performed for alkanes as long as *n*-hexane,² and new methodologies have been recently described³ to determine diffusivities of chains as long as C₂₀ in silicalite (structure type MFI⁴). These simulations were found to predict diffusivities more in line with microscopic experiments than with macroscopic measurements.

Up to now, the QENS technique has been mainly used to study translational dynamics in 3D systems: methane,⁵ ethane,⁶ and benzene⁷ in NaX and NaY zeolites, and methane⁸ and hydrogen⁹ in NaA. In the MFI structure, the two intersecting channel system leads to diffusion anisotropy, the straight

channels run along the *y* axis, and sinusoidal channels run along the *x* axis. Diffusion in the *z* direction can only be achieved via alternating migration in the *x* and *y* directions. The experimentally measured anisotropy factor (1/2)(D_{*x*} + D_{*y*})/D_{*z*} was found to be close to 5.¹⁰ The diffusion of methanol¹¹ and of a series of *n*-alkanes, methane, ethane, propane, butane, and hexane,^{12–14} was studied by QENS in the MFI structure, but only the mean diffusivity could be extracted from the data.

In Na-mordenite (structure type MOR⁴), the influence of one-dimensional diffusion on the QENS profiles of diffusing benzene was recognized,¹⁵ but the calculated curves were almost indistinguishable from the usual Lorentzian profiles that are observed for isotropic diffusion. This was due to the resolution of the spectrometer, which was not high enough, or alternatively to the slow mobility of benzene. Another attempt was made in the MOR structure by measuring methane diffusion.¹⁶ However, a large proportion of methane molecules were found to be trapped in the side pockets, in agreement with Monte Carlo simulations.¹⁷ The weak signal due to molecules diffusing in the channels did not justify an analysis of the data in terms of anisotropic diffusion.

In order to measure only one-dimensional diffusion and possibly single-file diffusion, two 1D structures without pockets were selected. Firstly, we have considered AlPO₄-5 since PFG NMR measurements have been carried out on this zeolite.^{18,19} In the literature, the value that is quoted for the free diameter of the cylindrical channels in AlPO₄-5 is 7.3 Å.⁴ It is based on an oxygen radius of 1.35 Å. However, recent experimental^{20,21} and simulation²² studies indicate that up to six methane molecules can be adsorbed per unit cell. The free diameter of AlPO₄-5 would then be much larger than the nominal value (it is estimated as 8.2 Å in ref 21 in the presence of methane molecules). The kinetic diameter of methane is 3.8 Å;²³ it is the intermolecular distance of closest approach for two mol-

* Author for correspondence.

[†] Institut de Recherches sur la Catalyse.

[‡] Universität Leipzig.

[§] Université Joseph Fourier.

^{||} Institut für Angewandte Chemie.

[⊥] Institut Laue-Langevin.

[⊗] Abstract published in *Advance ACS Abstracts*, July 1, 1997.

ecules colliding with zero initial kinetic energy.²³ Therefore, methane molecules could pass each other in this structure. Unidirectional but otherwise ordinary diffusion along the channel axis has indeed been found in recent MD simulations for methane in this structure.²⁴ On the other hand, larger molecules such as cyclopropane have no possibility at all to change their relative order during the observation time. Transport under these conditions has been termed single-file diffusion,^{25,26} and it is expected to have a profound influence on catalytic reaction rates since a molecule can only be desorbed after all other molecules adsorbed up to the channel orifice have diffused away.^{26–29} In order to test the concept that a tight fit between the size of the molecule and the dimension of the channel might enhance the mobility,³⁰ a second structure was chosen, ZSM-48. This high-silica zeolite has linear 10-ring channels with smaller dimension: $5.3 \times 5.6 \text{ \AA}$.³¹

QENS results are reported here on the diffusivities of methane, ethane, and cyclopropane in $\text{AlPO}_4\text{-5}$. The scattering function for ordinary 1D diffusion exists, but single-file diffusion has not been yet studied theoretically in neutron scattering. We have therefore derived the incoherent scattering function for the single-file diffusion model. Additional results obtained on methane diffusion in ZSM-48 are also presented. In this structure, it is impossible for methane molecules to pass each other. Since single-file diffusion has a larger sorbate concentration dependence compared to ordinary diffusion, it was preferred to vary the loading rather than the temperature during the limited allocated beam-time.

Experimental Section

Neutron Spectrometer. The neutron experiments were carried out at the Institut Laue-Langevin, Grenoble, using the time-of-flight (TOF) spectrometer IN5. This spectrometer has a good resolution, it covers the low-momentum transfer region, and it has a reasonable neutron flux. Since the calculated energy profile for single-file diffusion has a very narrow peak but very broad wings (vide infra), a large dynamic range is also required. The incident neutron wavelength was taken as 9.0 \AA (1.01 meV). This is a compromise between a long wavelength giving higher resolution and a small wavelength giving higher flux. In our case, the elastic resolution is $18 \mu\text{eV}$ (full-width at half-maximum). After scattering by the sample, neutrons are analyzed in 1000 ^3He detector tubes as a function of time and angle. The TOF of the scattered neutrons is related to their energy transfer and the scattering angle to the momentum transfer. Spectra from different detectors are grouped to obtain adequate counting statistics, excluding the Bragg peaks and the small-angle scattering from the zeolite. The TOF spectra were transformed to an energy scale after subtracting the scattering of the bare zeolite.

Samples. Almost single crystals of $\text{AlPO}_4\text{-5}$ ($20 \mu\text{m}$) were prepared using microwave heating during synthesis.³² Larger crystals of this aluminophosphate could have been prepared using the same method, but it was found that crystallization from a diluted gel yielded slightly smaller but very uniform crystals low in defects. The crystals were calcined at 973 K . For the neutron experiment, 2.2 g were used.

The ZSM-48 sample was synthesized hydrothermally using hexamethonium hydroxide, $\text{HM}(\text{OH})_2$, as templating agent. Typically, 0.3 mL of tetraethyl orthosilicate (TEOS, Aldrich) was hydrolyzed with 60 mL of a 1 M solution of $\text{HM}(\text{OH})_2$ for about 30 min with stirring. Distilled water (60 mL) was then added, and the temperature was increased to 353 K . The mixture was kept at this temperature for 2 h with stirring and the precursor gel, with the composition $\text{SiO}_2\text{-}0.2\text{HM}(\text{OH})_2\text{-}$

$20\text{H}_2\text{O}$, was transferred into an autoclave and heated at 453 K with stirring (300 rpm , magnetic stirrer) for 3 days . The autoclave was then cooled and the solid recovered by centrifugation. After washing with distilled water, the zeolite was dried at 383 K overnight and calcined at 823 K in air for 10 h . X-ray diffraction indicated that the zeolite was pure ZSM-48 without any extra phases. Crystals were in the form of elongated needles of dimension ca. $2 \times 0.1 \mu\text{m}$.

The samples were degassed to 10^{-3} Pa , at 700 K . They were transferred, inside a glovebox, into slab-shaped aluminum containers. Since the two zeolites do not contain protons, the neutron transmission of the dehydrated samples was excellent, $\approx 99\%$. The cells were connected to a gas inlet system so that adsorption could be performed in situ, even at low temperature. The estimated accuracy on the loadings determined during the neutron experiments is 20% .

Gravimetric Adsorption. The measurements were made on an electronic Sartorius microbalance, with a resolution of $10 \mu\text{g}$. Gas pressure was recorded by MKS Baratron capacitive gas pressure sensors. While recording the isotherms of cyclopropane in $\text{AlPO}_4\text{-5}$, we tried to desorb cyclopropane at room temperature over 15 h in the apparatus, at 10^{-3} Torr . This was not possible; the reason is not known (slow diffusion or residues). Therefore, a new calcination of the $\text{AlPO}_4\text{-5}$ crystals was performed out of the apparatus after each isotherm.

Theory of Neutron Scattering

For hydrogenous molecules, the incoherent scattering from hydrogen dominates. The measured intensity is proportional to the incoherent scattering function, $S_{\text{inc}}(\mathbf{Q}, \omega)$, which is the space and time Fourier transform of a self-correlation function, $G_s(\mathbf{r}, t)$:³³

$$S_{\text{inc}}(\mathbf{Q}, \omega) = (1/2\pi) \int \int d\mathbf{r} dt \exp[i(\mathbf{Q}\cdot\mathbf{r} - \omega t)] G_s(\mathbf{r}, t) \quad (1)$$

In our case, the self-correlation function, also called propagator in NMR, is the probability density to find a hydrogen atom at position \mathbf{r} at time t if the same atom was at the origin at time zero. The hydrogen atoms of the different adsorbates experience several molecular motions: translation, rotation, and vibration. The usual approximation is to consider that the molecular motions are uncoupled and can be treated separately. The total scattering function is then the convolution product of the individual scattering functions:

$$S_{\text{inc}}(\mathbf{Q}, \omega) = S_{\text{inc}}^{\text{trans}}(\mathbf{Q}, \omega) \otimes S_{\text{inc}}^{\text{rot}}(\mathbf{Q}, \omega) \otimes S_{\text{inc}}^{\text{vib}}(\mathbf{Q}, \omega) \quad (2)$$

where $\hbar\mathbf{Q}$ is the neutron momentum transfer. It is defined as $\mathbf{Q} = \mathbf{k} - \mathbf{k}_0$, where \mathbf{k} and \mathbf{k}_0 are the scattered and incident wave vectors, respectively. Similarly, $\hbar\omega$ is the neutron energy transfer; we limit our analysis to the range $\pm 0.4 \text{ meV}$. Since this energy transfer is too small to excite the internal vibrational modes of the molecules studied here, the vibrational term in eq 2 consists only in a Debye–Waller factor which has the effect of decreasing the intensity of the spectra at increasing Q values.

To describe the rotational behavior of methane and cyclopropane, the isotropic rotational diffusion model is well adapted; this model has already been used for methane adsorbed in ZSM-5.¹² For ethane, a less isotropic model, in which the molecules perform continuous rotational diffusion about the main molecular axis, is more adapted; this model was used in the case of ethane adsorption in ZSM-5.¹³

The most interesting part is the translational scattering function. The normal 1D diffusion and the single-file diffusion will be examined separately.

Normal 1D Diffusion. Let us consider a molecule diffusing in a 1D channel, with a diffusion coefficient D . If this channel makes an angle θ with the direction of \mathbf{Q} , the scattering function for this particular channel will be¹⁵

$$S_{1D}(\mathbf{Q}, \omega) = (1/\pi) D Q^2 \cos^2 \theta / [\omega^2 + (D Q^2 \cos^2 \theta)^2] \quad (3)$$

Since our samples are not oriented, one must perform a powder average of $S(\mathbf{Q}, \omega)$, which yields

$$S_{1D}(Q, \omega) = (1/2\pi) \int_0^\pi d\theta D Q^2 \cos^2 \theta \sin \theta / [\omega^2 + (D Q^2 \cos^2 \theta)^2] \quad (4)$$

Integration leads to the following expression:

$$S_{1D}(Q, \omega) = \frac{1}{4\pi\sqrt{2}\omega y} \left\{ \ln \left(\frac{1 + y^2 - \sqrt{2}y}{1 + y^2 + \sqrt{2}y} \right) + 2 \arctan(1 + \sqrt{2}y) - 2 \arctan(1 - \sqrt{2}y) \right\}$$

with

$$y^2 = D Q^2 / \omega \quad (5)$$

The same expression is obtained when considering a sample of isotropically distributed 1D channels.³⁴ In both cases, S_{1D} becomes infinite at $\omega = 0$. Experimentally however, there is no discontinuity because of the finite energy resolution. The simplest way to consider this influence is to convolute eq 3 with the instrumental resolution and then to perform the powder average numerically. The resulting curve is far from the Lorentzian found for 3D diffusion. However, in order to show this effect, the experimental resolution must be high enough. This is illustrated in Figure 1 for typical values of the parameters: $D = 10^{-8} \text{ m}^2 \text{ s}^{-1}$ and $Q = 0.3 \text{ \AA}^{-1}$. It is demonstrated in Figure 1a that for a sufficiently high energy resolution (triangular, fwhm = 0.2 \mu eV) a narrow component is present. With the energy resolution corresponding to our experimental conditions (triangular, fwhm = 18 \mu eV), one obtains the profile shown in Figure 1b as a solid line. It is close to a Lorentzian convoluted with the same resolution, Figure 1b, dotted line, so that good statistics are required to differentiate 1D from 3D diffusion.

Single-File Diffusion. The self-correlation function for a particle following single-file diffusion has already been derived.^{35,36} For a given channel, the self-correlation function was found to be

$$G_S(\mathbf{r}, t) = \frac{1}{\sqrt{2\pi\langle\sigma^2\rangle}} \exp\left(-\frac{r^2}{2\langle\sigma^2\rangle}\right) \quad (6)$$

The mean-square displacement of the particle, $\langle\sigma^2\rangle$, varies in proportion to $t^{1/2}$:

$$\langle\sigma^2\rangle = 2Ft^{1/2} \quad (7)$$

where F is the single-file mobility factor.²⁶ In the case of normal diffusion, the mean-square displacement is proportional to t . Comparisons have been made with PFG NMR measurements and with MD simulations.³⁷ A priori, the long-range mobility should be reduced in single-file systems compared with normal diffusion because of increased correlations between the molecules. For the same reason, a higher loading dependence is expected for single-file diffusion; indeed, F was found to be proportional to $(1 - \theta)/\theta$.²⁶ Therefore, experimental results

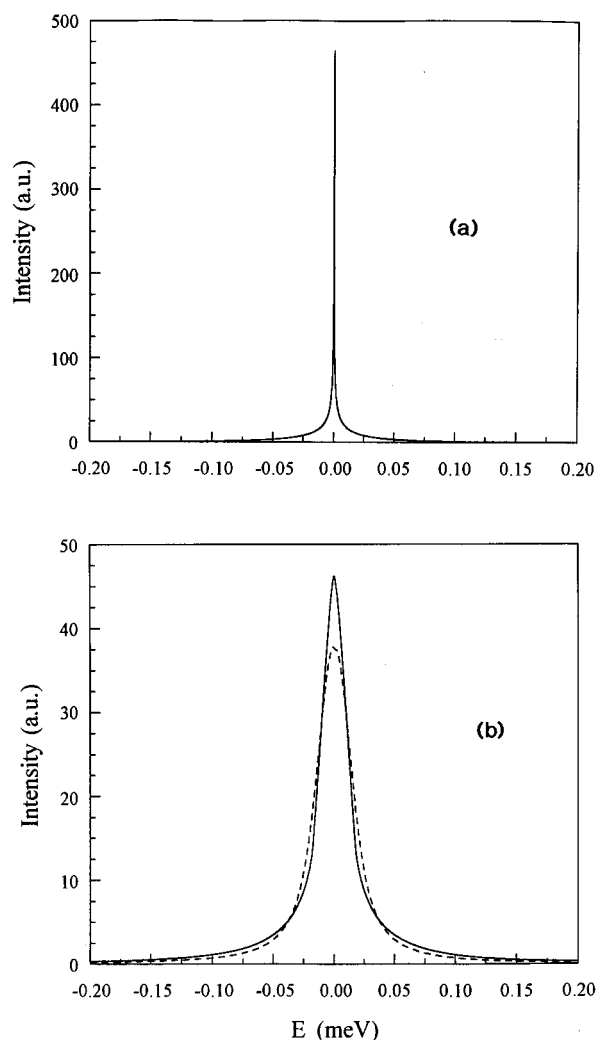


Figure 1. Simulated QENS spectra in the case of normal 1D diffusion for the following parameters: $D = 10^{-8} \text{ m}^2 \text{ s}^{-1}$, $Q = 0.3 \text{ \AA}^{-1}$. The scattering function is convoluted with a triangular resolution function of different full-width at half-maximum: (a) 0.2 \mu eV , (b) 18 \mu eV (solid lines). The broken line in part b corresponds to a pure Lorentzian profile.

claiming single-file behavior, including QENS, should show this strong loading dependence.

In order to derive the scattering function for single-file diffusion, one has to take the Fourier transform of the self-correlation function with respect to space and time. As in the normal 1D diffusion case, a particular channel making an angle θ with the direction of \mathbf{Q} will be considered. Firstly, space Fourier transformation leads to an intermediate scattering function

$$I_{SF}(\mathbf{Q}, t) = \int d\mathbf{r} G_S(\mathbf{r}, t) \exp(i\mathbf{Q}\cdot\mathbf{r}) = \exp(-FQ^2 \cos^2 \theta t^{1/2}) \quad (8)$$

An important difference with the case of normal diffusion lies in the term $t^{1/2}$ instead of t . After performing the powder average, the Fourier transform of $I(\mathbf{Q}, t)$ with respect to time gives the scattering function

$$S_{SF}(Q, \omega) = \frac{1}{\pi} \int_0^\pi d\theta \sin \theta \int_0^\infty dt \exp(-FQ^2 \cos^2 \theta t^{1/2}) \cos(\omega t) \quad (9)$$

Integrating over t , one obtains³⁸

$$S_{\text{SF}}(Q, \omega) = \frac{FQ^2\omega^{-3/2}}{\sqrt{2\pi}} \int_0^\pi d\theta \cos^2 \theta \sin \theta \left[\cos\left(\frac{\pi z^2}{2}\right) \left(\frac{1}{2} - C(z)\right) + \sin\left(\frac{\pi z^2}{2}\right) \left(\frac{1}{2} - S(z)\right) \right]$$

where

$$z^2 = \frac{F^2 Q^4 \cos^4 \theta}{2\pi\omega} \quad (10)$$

C and S are the Fresnel integrals as defined in ref 39 (7.3.3 and 7.3.4). Following ref 39, the term in brackets in eq 10 is denoted as

$$g(z) = \cos\left(\frac{\pi z^2}{2}\right) \left(\frac{1}{2} - C(z)\right) + \sin\left(\frac{\pi z^2}{2}\right) \left(\frac{1}{2} - S(z)\right) \quad (11)$$

For $g(z)$, the rational approximation³⁹

$$g(z) = \frac{1}{2 + 4.142z + 3.492z^2 + 6.670z^3} + \epsilon(z) \quad (12)$$

can be used, where the absolute error of this approximation is

$$|\epsilon(z)| \leq 2 \times 10^{-3} \quad (13)$$

The scattering function then becomes

$$S_{\text{SF}}(Q, \omega) = \frac{2\pi}{F^2 Q^4} \int_0^\pi \frac{z^3 \sin \theta d\theta}{\cos^4 \theta (2 + 4.142z + 3.492z^2 + 6.67z^3)} \quad (14)$$

Again, powder averaging and convolution with a resolution function have a great influence on the spectral profile. With the parameters $F = 10^{-11} \text{ m}^2 \text{ s}^{-1/2}$ and $Q = 0.3 \text{ \AA}^{-1}$, one obtains the QENS spectrum shown in Figure 2a, after convolution with a narrow energy resolution function (triangular, fwhm = 0.2 μeV). The peak is even sharper than in the normal 1D diffusion case. With the actual energy resolution (triangular, fwhm = 18 μeV), the profile is still found to be sharp; cf. the solid line in Figure 2b. In contrast to the case of ordinary 1D diffusion, the more waisted peak shape cannot be fitted with a Lorentzian, dotted line in Figure 2b. Analytical expressions of the scattering function, for different resolution functions (triangular, Gaussian, and Lorentzian) will be presented elsewhere.³⁴

It should be stressed that the time scale of the measurement has a prominent effect on the observed diffusion regime. In PFG NMR, one is always concerned with the long-time limit so that single-file diffusion as characterised by eq 7 is observed. In our QENS experiment, broadenings as large as 1 meV or down to 10% of the resolution can be resolved so that the time scale is in the range 1–350 ps. On this time scale, the diffusion can follow normal 1D diffusion at low loadings since correlations between molecules can be neglected, but at high loadings single-file diffusion could be measured.

Results

Methane in AlPO₄-5. QENS measurements were performed at 155 K, for the two methane concentrations of 0.7 and 1 molecule per unit tube length (8.417 \AA^{40}). Higher loadings were not considered to avoid signal from the gas phase.

At both loadings, all the QENS spectra could be fitted simultaneously with normal 1D diffusion convoluted with isotropic rotation and with the instrumental resolution. The agreement between experimental and calculated spectra is reasonable, as shown in Figure 3. The agreement is better with

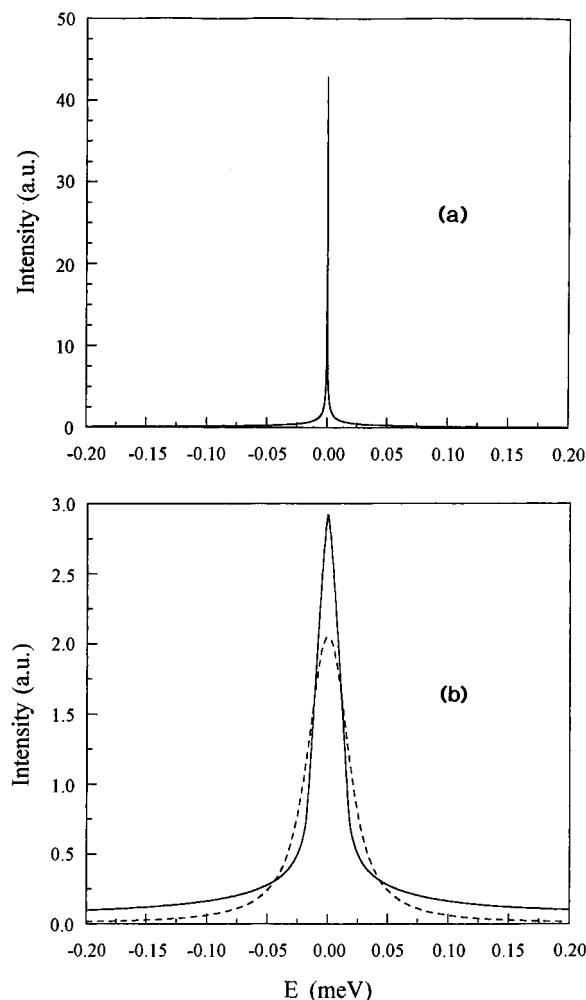


Figure 2. Simulated QENS spectra in the case of single-file diffusion for the following parameters: $F = 10^{-11} \text{ m}^2 \text{ s}^{-1/2}$, $Q = 0.3 \text{ \AA}^{-1}$. The scattering function is convoluted with a triangular resolution function of different full-width at half-maximum: (a) 0.2 μeV , (b) 18 μeV (solid lines). The broken line in part b corresponds to a pure Lorentzian profile.

1D than with 3D diffusion (the sum of residuals is smaller). The spectra cannot be fitted with the single-file diffusion model. The decrease of intensity of the spectra with increasing Q values is due to the Debye–Waller factor. The diffusion coefficients for methane are $1.6 \times 10^{-9} \text{ m}^2 \text{ s}^{-1}$ for a concentration of 0.7 molecule/unit cell and $1.2 \times 10^{-9} \text{ m}^2 \text{ s}^{-1}$ for a concentration of 1 molecule/unit cell. The concentration dependence of the diffusion coefficient is thus found to be rather moderate (the experimental error is $\approx 50\%$). At the two loadings used, the molecules cannot be considered to be isolated, especially at small Q values corresponding to large diffusion paths. The first grouping of detectors has a mean Q value of 0.19 \AA^{-1} so that translation is measured over a distance $\lambda = 2\pi/Q$ of 33 \AA , corresponding to 4 unit cells. It appears therefore that methane molecules are able to cross each other in AlPO₄-5 and single-file diffusion is not observed.

Ethane in AlPO₄-5. The diffusion of ethane was studied at 250 K and at loadings of 0.8, 1.4, and 1.6 molecules per unit cell (uc).

For all loadings, the QENS spectra could be fitted simultaneously with normal 1D diffusion convoluted with uniaxial rotation and with the instrumental resolution. Experimental and calculated spectra are shown in Figure 4 for the medium loading; the agreement is quite good. As in the case of methane, the spectra cannot be fitted with the single-file diffusion model and the agreement is better with 1D than with 3D diffusion. The

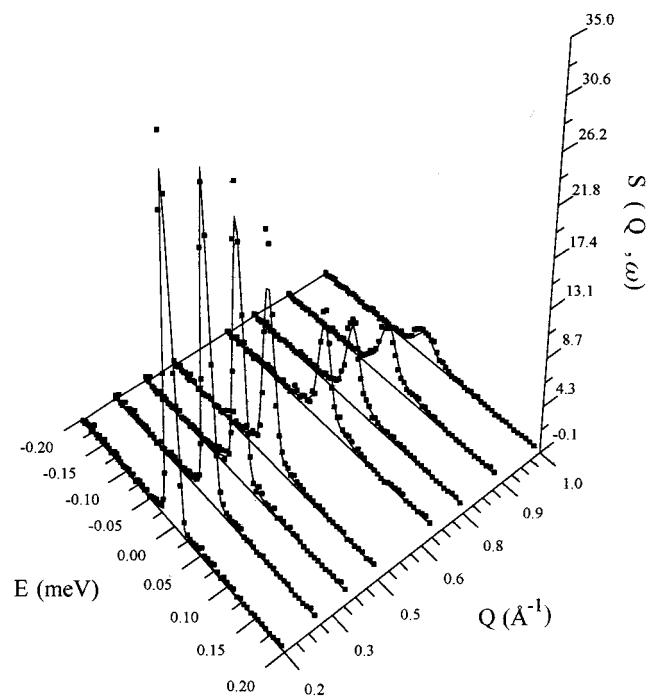


Figure 3. QENS spectra, obtained at different values of the momentum transfer Q , for methane adsorbed in $\text{AlPO}_4\text{-5}$ (concentration of 1 molecule per unit cell, $T = 155$ K): (■) experimental points, (—) profile calculated with the normal 1D diffusion model.

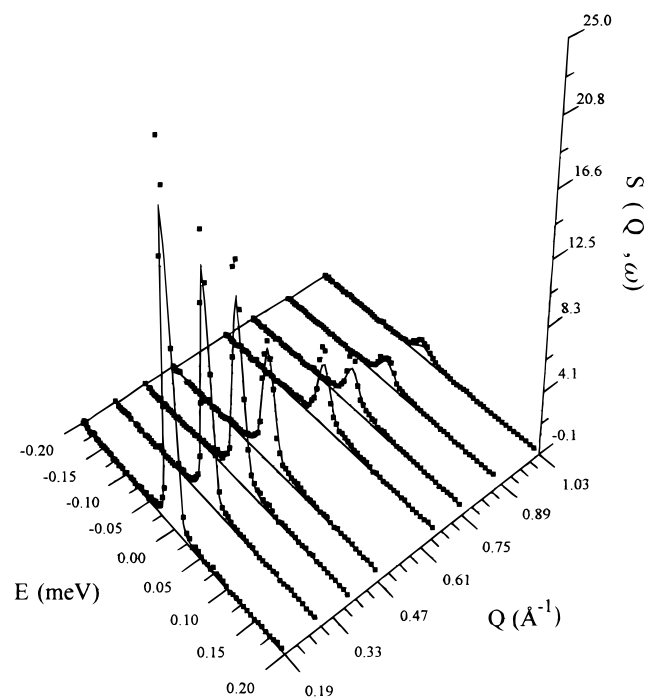


Figure 4. QENS spectra, obtained at different values of the momentum transfer Q , for ethane adsorbed in $\text{AlPO}_4\text{-5}$ (concentration of 1.4 molecule per unit cell, $T = 250$ K): (■) experimental points, (—) profile calculated with the normal 1D diffusion model.

diffusion coefficients of ethane are $1.4 \times 10^{-9} \text{ m}^2 \text{ s}^{-1}$ for a concentration of 0.7 molecule/uc, $1.1 \times 10^{-9} \text{ m}^2 \text{ s}^{-1}$ for 1.4 molecule/uc, and $9.0 \times 10^{-10} \text{ m}^2 \text{ s}^{-1}$ for 1.6 molecule/uc, respectively. Again, the concentration dependence of the diffusion coefficient is only moderate. As for methane, the evidence of ordinary 1D diffusion indicates that ethane molecules are able to pass each other in $\text{AlPO}_4\text{-5}$. In view of the similarity of the kinetic diameters of these two molecules, this finding does not seem to be unreasonable.

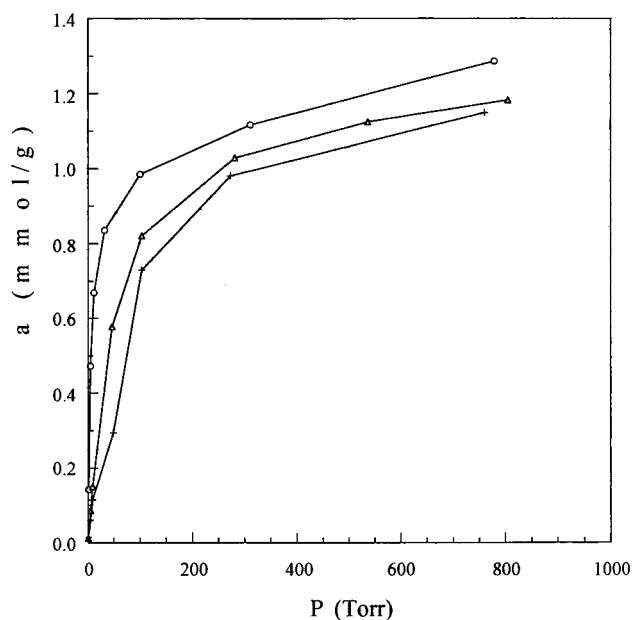


Figure 5. Adsorption isotherms for cyclopropane in $\text{AlPO}_4\text{-5}$: $T = 250$ K (○), 273 K (▽), and 306 K (+).

Cyclopropane in $\text{AlPO}_4\text{-5}$. QENS spectra were measured at 273 K, at concentrations of 0.6 and 1.3 molecule/uc. Isotherms obtained at different temperatures are shown in Figure 5.

Only the spectra obtained at low loading showed a significant broadening. All the spectra could be fitted simultaneously with normal 1D diffusion, convoluted with isotropic rotation and with the instrumental resolution. The fit is better with 1D than with 3D diffusion. A comparison between the experimental and calculated spectra for $Q = 0.39 \text{ \AA}^{-1}$ is shown in Figure 6a. At this Q value, there is a large broadening due to normal 1D diffusion, and only 14% of the signal is due to rotation. The spectrum cannot be fitted with the single-file diffusion model. The diffusion coefficient for cyclopropane at this loading is $1.8 \times 10^{-9} \text{ m}^2 \text{ s}^{-1}$.

At higher loading, the spectrum corresponding to the same Q value shows only an elastic peak, as can be seen from Figure 6b. In the case of ethane, for an even larger number of molecules per unit cell, a broadening was observed and the diffusion was found to follow normal 1D diffusion. For cyclopropane, the elastic response at high loading can only be explained by single-file diffusion, indicating that the molecules cannot pass each other in $\text{AlPO}_4\text{-5}$. We believe that single-file diffusion can only be inferred if there is such a large loading dependence of the diffusivity. However, the mobility is too small to be determined with this resolution. Fits of the spectra with eq 14 indicate that the mobility factor F is smaller than $10^{-12} \text{ m}^2 \text{ s}^{-1/2}$. A broadening is measured at higher Q values, but one has to then take into account the contribution due to the rotation.

Methane in ZSM-48. The previous system gives some evidence that single-file diffusion is occurring, but it is impossible to extract a mobility factor. Methane in ZSM-48 was selected to obtain additional results on single-file diffusion and to test whether the mobility of methane would be enhanced compared with $\text{AlPO}_4\text{-5}$, due to the better fit between the size of the molecule and the size of the channel. QENS measurements were first made at 100 K, close to saturation capacity (≈ 1.2 molecule per unit length tube). Under these conditions, no long-range mobility could be observed. The temperature was then raised to 155 K, and three different loadings were studied. The isotherm at 155 K was measured volumetrically

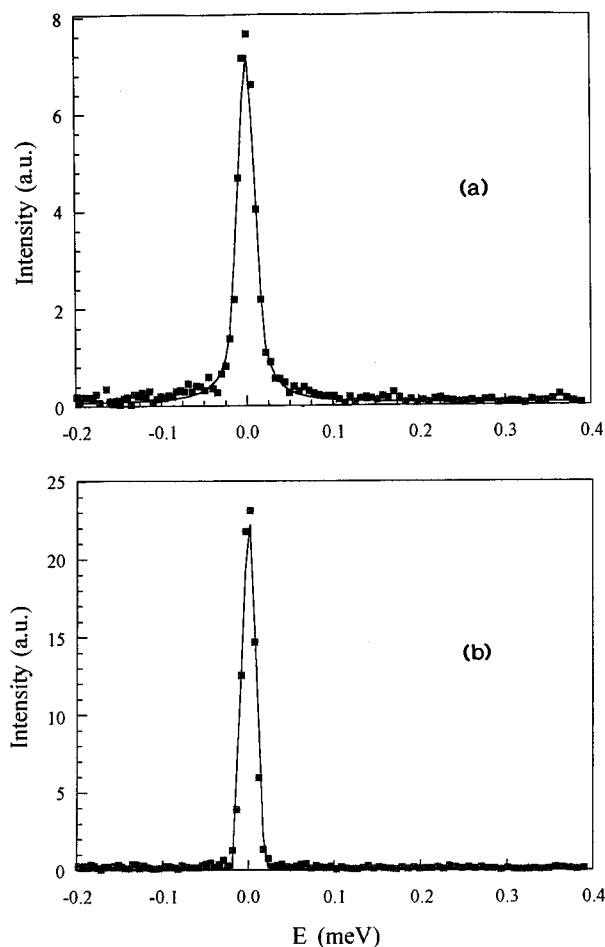


Figure 6. Comparison of experimental (■) and calculated (—) QENS spectra obtained at 273 K for cyclopropane adsorbed in AIPO₄-5: (a) 0.6 molecule per unit cell, profile calculated with the normal 1D diffusion model; (b) 1.3 molecule per unit cell, profile calculated with the single-file diffusion model ($Q = 0.39 \text{ \AA}^{-1}$).

during the neutron experiment so that the relative pore occupancies could be derived.

At low methane loading, $\theta = 0.11$, a large broadening was observed. All the spectra could be fitted simultaneously with normal 1D diffusion, convoluted with isotropic rotation and with the instrumental resolution. The fit is better with 1D than with 3D diffusion. An example for the comparison between an experimental and calculated spectrum, for $Q = 0.35 \text{ \AA}^{-1}$, is shown in Figure 7a. This spectrum cannot be fitted with the single-file diffusion model. At this Q value, only 5% of the signal comes from the rotation so that one can be confident that the measured broadening is due to diffusion. For this loading, the diffusion coefficient of methane is $2.5 \times 10^{-9} \text{ m}^2 \text{ s}^{-1}$, which is not much larger than the value obtained in AIPO₄-5. Therefore, there is no indication of supermobility. In ZSM-5, the value of the diffusion coefficient extrapolated at 155 K is close to $10^{-9} \text{ m}^2 \text{ s}^{-1}$,¹² so that the diffusivity of methane in these three zeolites is similar and does not depend on the size of the channel.

For a higher loading, $\theta = 0.48$, the spectrum obtained at the same Q value is completely different, as can be seen in Figure 7b. The large loading dependence of the diffusivity of methane, which was not observed in AIPO₄-5, indicates that single-file diffusion is observed for this molecule in ZSM-48. The evidence is provided by the quasi-elastic foot in Figure 7b, which cannot be fitted adequately by a Lorentzian function. The mobility factor, obtained by fitting the spectra with eq 14, is $2 \times 10^{-12} \text{ m}^2 \text{ s}^{-1/2}$. Since the quasi-elastic intensity is weak and

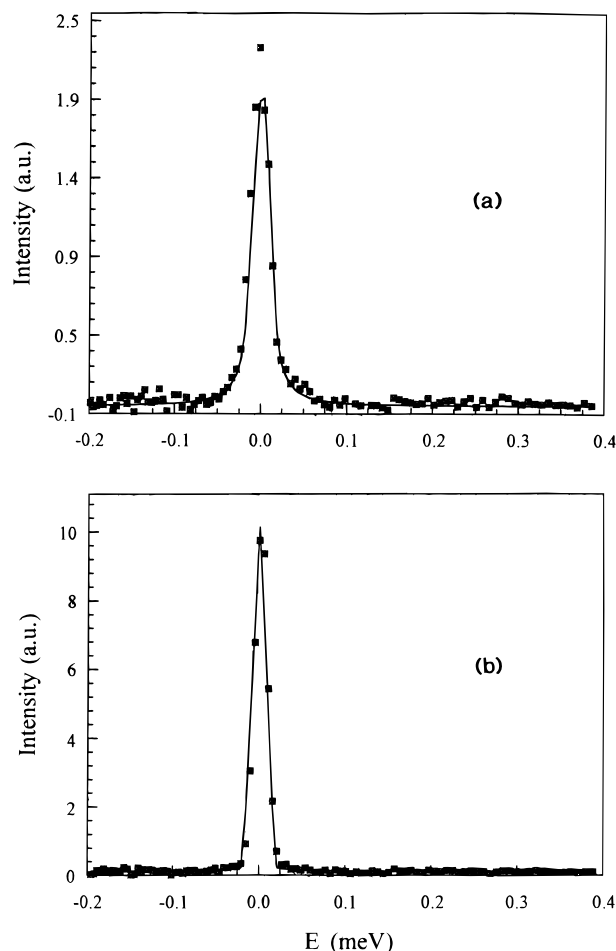


Figure 7. Comparison of experimental (■) and calculated (—) QENS spectra obtained at 155 K for methane adsorbed in ZSM-48: (a) $\theta = 0.11$, profile calculated with the normal 1D diffusion model; (b) $\theta = 0.48$, profile calculated with the single-file diffusion model ($Q = 0.35 \text{ \AA}^{-1}$).

since the rotational contribution has been neglected, the value of the mobility factor is only an estimation. It is an upper limit. Larger values would be easier to measure since the quasi-elastic broadening would be larger. One may note that only large single-file diffusivities can be measured with microscopic techniques: QENS or PFG NMR.

At $\theta = 0.8$, the signal is perfectly elastic, like in Figure 6b. At this loading, the mobility factor is therefore less than $10^{-12} \text{ m}^2 \text{ s}^{-1/2}$.

Discussion

In the present study, QENS has been successfully applied for the first time to confirm the occurrence of single-file diffusion in zeolites with unidimensional channel structure. Although the experimental error is large, best fits of the QENS data for methane in ZSM-48, at medium loading, have been obtained with the single-file model of proportionality between the mean-square displacement of the molecule and the square root of the observation time, in complete agreement with the theoretical predictions, eq 7. On the other hand, at low loading, the measurements indicate proportionality between the mean-square displacement and the observation time corresponding to normal 1D diffusion.

The crossover between the two cases may be easily attributed to the change in the relation between the mean free distance l between the adsorbed molecules and the space scale λ of the present QENS experiments ($\lambda = 18 \text{ \AA}$ for the spectra shown in Figure 7).

The mean free distance l between methane molecules can be derived from the relation⁴¹

$$l = \frac{1 - \theta}{\theta} \sigma \quad (15)$$

where σ is the kinetic diameter of the methane molecule.

For a medium concentration, $\theta = 0.48$, l is equal to 4 Å, and thus $l < \lambda$. In this case, the mutual encounters between adjacent diffusants become relevant, ensuring the necessary condition for single-file behavior.

For a small concentration, $\theta = 0.11$, l is equal to 31 Å, and thus $l > \lambda$. Molecular diffusion is then essentially unaffected by the other molecules. Depending on the rate of momentum and energy exchange with the zeolite lattice, molecular propagation can be described by the ballistic stage or, for sufficiently fast momentum exchange, by ordinary diffusion.³⁷

It is possible to relate the single-file mobility factor, F , with a diffusivity that could be measured at infinitely small concentration, D_i .^{41,42} The expression derived by Hahn and co-workers⁴¹ is simply

$$D_i = \pi \frac{F^2}{l^2} \quad (16)$$

For methane in ZSM-48, at medium concentration, F was found to be $2 \times 10^{-12} \text{ m}^2 \text{ s}^{-1/2}$. Using eq 16, this gives a value of $7 \times 10^{-5} \text{ m}^2 \text{ s}^{-1}$ for D_i , which would be in striking contrast to the diffusion coefficient $D = 2.5 \times 10^{-9} \text{ m}^2 \text{ s}^{-1}$, directly measured for $\theta = 0.11$. The diffusivity of an isolated molecule would then be more than 4 orders of magnitude larger than the diffusivity derived for $\theta = 0.11$. This discrepancy could be due to the fact that mutual collisions of the molecules occur already for $\theta = 0.11$. Additional measurements are planned, with a better elastic resolution, to measure single-file diffusion with a better accuracy.

In the more open 1D channel system of AlPO₄-5, best fits between the experimentally observed scattering behavior and transport models have been obtained with normal 1D diffusion, for methane and ethane. It appears that the experimental and simulation results reported so far in the literature about the transport properties of the light alkanes in AlPO₄-5 are in disagreement. For methane, the PFG NMR measurements of Kukla et al. were interpreted by a single-file diffusion model,¹⁸ whereas according to another study methane is found to conform to normal 1D diffusion.¹⁹ Quite recently, ordinary 1D diffusion was found by Martin et al. using QENS.⁴³ The diffusion coefficient reported by Nivarthi et al. is $2.9 \times 10^{-9} \text{ m}^2 \text{ s}^{-1}$ at 300 K, which is in keeping with our value of $1.6 \times 10^{-9} \text{ m}^2 \text{ s}^{-1}$, at 155 K, for the same concentration of 0.7 molecule/uc. For larger loadings, the diffusion coefficient derived from the other QENS experiment⁴³ is $1.0 \times 10^{-9} \text{ m}^2 \text{ s}^{-1}$, at 97 K, for 1.2 molecule/uc, in good agreement with our value of $1.2 \times 10^{-9} \text{ m}^2 \text{ s}^{-1}$, obtained at 155 K for 1 molecule/uc. We note that recent MD simulations for methane in this structure²⁴ are also in favor of ordinary 1D diffusion. However, it is also found in this work²⁴ that ethane molecules cannot pass each other easily and exhibit a mobility in between single-file and normal 1D diffusion. Experimentally, the same group has found by PFG NMR that ethane molecules follow single-file diffusion,⁴² while our present QENS results suggest ordinary 1D diffusion. For cyclopropane, we find that this molecule follows single-file diffusion. This could be the reason for the slow desorption rates observed during the gravimetric measurements. This molecule would correspond to the simulation made by Keffer

et al.²⁴ for a slightly larger molecule ($\sigma = 5 \text{ Å}$) showing pure single-file diffusion in AlPO₄-5.

The explanation we offer for the experimental discrepancies is that the observation or nonobservation of single-file diffusion decisively depends on the real structure of the adsorbent under study. In all these studies, different AlPO₄-5 crystals have been used. It is mentioned in ref 20 that some samples adsorbed 4 molecules/uc, but others 6 molecules/uc. It is also known that the crystallinity of this material deteriorates with time and water moisture⁴⁴ and that the calcination procedure must be slow enough to avoid defects or partial collapse of the structure.

To explain the discrepancy between our QENS results for ethane and the MD investigation,²⁴ one may speculate that the results of MD simulations in this particular structure will be affected by subtle changes of the potential, as shown in ref 22. Furthermore, the simulations were performed with a rigid framework, neglecting the influence of lattice vibrations, which might have an effect for such a limiting case.

Conclusion

Two different diffusion regimes have been measured with the quasi-elastic neutron scattering technique, by varying the concentration of molecules in 1D channel structures. Ordinary 1D diffusion is observed at low loading for cyclopropane in AlPO₄-5 and for methane in ZSM-48. At higher loadings, single-file diffusion is found for both systems. The crossover between the two regimes is attributed to the variation of the mean free distance between molecules with respect to the space scale of the present QENS experiments. Ordinary 1D diffusion is observed for methane and ethane in AlPO₄-5, whatever the loading. It is probable that the different origin of the samples explains the discrepancies found with PFG NMR results in this aluminophosphate. Comparative studies with identical sample materials are thus required. In ZSM-48, the mobility factor of methane at medium concentration is $2 \times 10^{-12} \text{ m}^2 \text{ s}^{-1/2}$. This yields a diffusivity for an isolated molecule more than 4 orders of magnitude larger than the diffusivity derived at low loading, which seems surprising. It is clear that the characterization of single-file diffusion is a fairly recent topic and that it deserves further studies.

Acknowledgment. The neutron experiments were performed at the Institut Laue-Langevin, Grenoble, France. Two of us, K.H. and J.K., are obliged to the Deutsche Forschungsgemeinschaft (Sonderforschungsbereich 294) for financial support. We also thank Dr. J. Caro, Institut für Angewandte Chemie-Berlin, for discussions.

References and Notes

- (1) Kärger, J.; Ruthven, D. M. *Diffusion in Zeolites and Other Microporous Solids*; Wiley: New York, 1992.
- (2) June, R. L.; Bell, A. T.; Theodorou, D. N. *J. Phys. Chem.* **1992**, *96*, 1051.
- (3) Maginn, E. J.; Bell, A. T.; Theodorou, D. N. *J. Phys. Chem.* **1996**, *100*, 7155.
- (4) Meier, W. M.; Olson, D. H.; Baerlocher, Ch., Eds. *Atlas of Zeolites Structure Types*; Elsevier: Amsterdam, Zeolites 17, 1996.
- (5) Jobic, H.; Bée, M.; Kearley, G. J. *J. Phys. Chem.* **1994**, *98*, 4660.
- (6) Jobic, H.; Bée, M.; Caro, J.; Bülow, M.; Kärger, J.; Pfeifer, H. In *Studies in Surface Science and Catalysis*; Ohlmann, G., Pfeifer, H., Fricke, R., Eds.; Elsevier: Amsterdam, 1991; Vol. 65, p 445.
- (7) Jobic, H.; Bée, M.; Kärger, J.; Pfeifer, H.; Caro, J. *J. Chem. Soc., Chem. Commun.* **1990**, 341.
- (8) Cohen de Lara, E.; Kahn, R. *J. Phys.* **1981**, *42*, 1029.
- (9) Kahn, R.; Cohen de Lara, E.; Viennet, E. *J. Chem. Phys.* **1989**, *91*, 5097.
- (10) Hong, U.; Kärger, J.; Kramer, R.; Pfeifer, H.; Seiffert, G.; Müller, U.; Unger, K. K.; Lück, H. B.; Ito, T. *Zeolites* **1991**, *11*, 816.

- (11) Jobic, H.; Renouprez, A.; Bée, M.; Poinssignon, C. *J. Phys. Chem.* **1986**, *90*, 1059.
- (12) Jobic, H.; Bée, M.; Kearley, G. J. *Zeolites* **1989**, *9*, 312.
- (13) Jobic, H.; Bée, M.; Kearley, G. J. *Zeolites* **1992**, *12*, 146.
- (14) Jobic, H.; Bée, M.; Caro, J. Proceedings 9th International Zeolite Conference, Montreal, 1992; von Ballmoos, R., Higgins, J. B., Treacy, M. M. J., Eds.; Butterworth-Heinemann: Boston, 1993; Vol. II, p 121.
- (15) Jobic, H.; Bée, M.; Renouprez, A. *Surf. Sci.* **1984**, *140*, 307.
- (16) Jobic, H.; Bée, M. *Z. Phys. Chem.* **1995**, *189*, 179.
- (17) Smit, B.; den Ouden, C. J. J. *J. Phys. Chem.* **1988**, *92*, 7169.
- (18) Kukla, V.; Kornatowski, J.; Demuth, D.; Girnus, I.; Pfeifer, H.; Rees, L. V. C.; Schunk, S.; Unger, K. K.; Kärger, J. *Science* **1996**, *272*, 702.
- (19) Nivarthi, S. S.; Mc Cormick, A. V.; Davis, H. T. *Chem. Phys. Lett.* **1994**, *229*, 297.
- (20) Coulomb, J. P.; Martin, C.; Grillet, Y.; Tosi-Pellenq, N. *Studies in Surface Science and Catalysis*; Proceedings 10th International Zeolite Conference, Garmisch-Partenkirchen, 1994; Weitkamp, J., Karge, H. G., Pfeifer, H., Hölderich, W., Eds.; Elsevier: Amsterdam, 1994; Vol. 84, p 445.
- (21) Martin, C.; Tosi-Pellenq, N.; Patarin, J.; Coulomb, J. P. *Langmuir*, accepted for publication.
- (22) Lachet, V.; Boutin, A.; Pellenq, R. J. M.; Nicholson, D.; Fuchs, A. *J. Phys. Chem.* **1996**, *100*, 9006.
- (23) Breck, D. W. *Zeolite Molecular Sieves*; Wiley: New York, 1974.
- (24) Keffer, D.; Mc Cormick, A. V.; Davis, H. T. *Mol. Phys.* **1996**, *87*, 367.
- (25) Hodkin, A. L.; Keynes, R. D. *J. Physiol. (London)* **1955**, *128*, 61.
- Riekert, L. *Adv. Catal.* **1970**, *21*, 281.
- (26) Kärger, J.; Petzold, M.; Pfeifer, H.; Ernst, S.; Weitkamp, J. *J. Catal.* **1992**, *136*, 283.
- (27) Lei, G. D.; Sachtler, W. M. H. *J. Catal.* **1993**, *140*, 601.
- (28) Rödenbeck, C.; Kärger, J.; Hahn, K. *J. Catal.* **1995**, *157*, 656.
- (29) Lei, G. D.; Carvill, B. T.; Sachtler, W. M. H. *Appl. Catal. A* **1996**, *141*, 347.
- (30) Derouane, E. G.; Andre, J. M.; Lucas, A. A. *J. Catal.* **1988**, *110*, 58.
- (31) Schlenker, J. L.; Rohrbaugh, W. J.; Chu, P.; Valyocsik, E. W.; Kokotailo, G. T. *Zeolites* **1985**, *5*, 355.
- (32) Girnus, I.; Jancke, K.; Vetter, R.; Richter-Mendau, J.; Caro, J. *Zeolites* **1995**, *15*, 33.
- (33) Bée, M. *Quasielastic Neutron Scattering*; Adam Hilger: Bristol, 1988.
- (34) Hahn, K.; Jobic, H.; Kärger, J. In preparation.
- (35) Kärger, J. *Phys. Rev. E* **1993**, *47*, 1427.
- (36) Hahn, K.; Kärger, J. *J. Phys. A: Math. Gen.* **1995**, *28*, 3061.
- (37) Hahn, K.; Kärger, J. *J. Phys. Chem.* **1996**, *100*, 316.
- (38) Prudnikov, A. P.; Brychkov, J. A.; Marichev, I. O. *Integrals and Series*; Nauka: Moscow, 1981.
- (39) Abramovitz, M.; Stegun, I. A. *Handbook of Mathematical Functions*; Dover Publications: New York, 1968.
- (40) Mora, A. J.; Fitch, A. N.; Cole, M.; Goyal, R.; Jones, R. H.; Jobic, H.; Carr, S. W. *J. Mater. Chem.* **1996**, *6*, 1831.
- (41) Hahn, K.; Kärger, J.; Kukla, V. *Phys. Rev. Lett.* **1996**, *76*, 2762.
- (42) Gupta, V.; Nivarthi, S. S.; McCormick, A. V.; Davies, H. T. *Chem. Phys. Lett.* **1995**, *247*, 596.
- (43) Martin, C.; Coulomb, J. P.; Grillet, Y.; Kahn, R. In *Fundamentals of Adsorption*; Le Van, M. D., Ed.; Kluwer Academic Publishers: Boston, 1996; p 587.
- (44) Hampson, B.; Leach, H. F.; Lowe, B. M.; Williams, C. D. *Zeolites* **1989**, *9*, 521.